

ALFVÉN WAVES IN SIMULATIONS OF SOLAR PHOTOSPHERIC VORTICES

S. SHELYAG¹, P. S. CALLY¹, A. REID², AND M. MATHIOUDAKIS²

¹ Monash Centre for Astrophysics, School of Mathematical Sciences, Monash University, Victoria 3800, Australia

² Astrophysics Research Centre, School of Mathematics and Physics, Queen's University Belfast, Belfast BT7 1NN, UK

Received 2013 July 21; accepted 2013 September 7; published 2013 September 23

ABSTRACT

Using advanced numerical magneto-hydrodynamic simulations of the magnetized solar photosphere, including non-gray radiative transport and a non-ideal equation of state, we analyze plasma motions in photospheric magnetic vortices. We demonstrate that apparent vortex-like motions in photospheric magnetic field concentrations do not exhibit “tornado”-like behavior or a “bath-tub” effect. While at each time instance the velocity field lines in the upper layers of the solar photosphere show swirls, the test particles moving with the time-dependent velocity field do not demonstrate such structures. Instead, they move in a wave-like fashion with rapidly changing and oscillating velocity field, determined mainly by magnetic tension in the magnetized intergranular downflows. Using time–distance diagrams, we identify horizontal motions in the magnetic flux tubes as torsional Alfvén perturbations propagating along the nearly vertical magnetic field lines with local Alfvén speed.

Key words: magnetohydrodynamics (MHD) – plasmas – Sun: magnetic fields – Sun: photosphere

Online-only material: animations, color figures

1. INTRODUCTION

Vortices in magnetic field concentrations in the simulated upper solar photosphere, first identified by Vögler (2004) and Vögler et al. (2005), have recently attracted a lot of interest. These structures have been suggested as a primary candidate mechanism for energy transport from the solar interior to the outer layers of the solar atmosphere (Wedemeyer-Böhm et al. 2012). Recently, Shelyag et al. (2011b) demonstrated that the major contributor to vertical vorticity in these photospheric magnetic field concentrations is magnetic tension in the low plasma β regions. Initial analysis of velocity fields in magnetic photospheric vortices demonstrated a complex multi-layered structure of oppositely rotating surfaces with nearly constant vorticity that are parallel to the magnetic field lines (Shelyag et al. 2011a; Fedun et al. 2011). Steiner & Rezaei (2012) found a similar behavior of the velocity field in the solar photospheric simulations carried out with CO5BOLD (Freytag et al. 2012). Poynting flux emerging from the simulated solar photosphere was linked to the horizontal plasma motions in the photospheric magnetic field (Shelyag et al. 2012). Moll et al. (2012) showed that vortex motions in the simulated photosphere are able to dissipate their energy and produce additional local heating of the solar chromosphere. Kitiashvili et al. (2013) suggested that small-scale solar atmospheric eruptions, such as spicules, are linked to horizontal vortex-like motions in photospheric magnetic flux tubes. Morton et al. (2013) observationally demonstrated excitation of incompressible waves in the solar chromosphere by photospheric vortex motions. Using multi-wavelength observations, it was recently demonstrated that these essentially magnetic structures extend from the lower photosphere to the corona, and are connected to the observed swirls in the solar chromosphere (Wedemeyer-Böhm & Ruppe van der Voort 2009) and lower coronal regions (Wedemeyer-Böhm et al. 2012).

In this Letter, using a time series of magnetized photospheric models produced by the MURaM code (Vögler et al. 2005), we further analyze the character of plasma motions in intergranular magnetic field concentrations. We demonstrate that,

if dependence of the local velocity field on time is taken into account, the apparent swirling motions in the strong magnetic field disappear, and swirls do not exist in photospheric magnetic flux tubes. Instead, a wave-like behavior is observed for horizontal motions of test particles following the time-dependent velocity field. The restoring force of magnetic tension acts as a conduit of oscillatory vorticity upward from deeper photospheric layers, where it is generated by convective motions. Using vertical-component-of-vorticity time–distance diagrams taken along a vertical axis we show that the vorticity perturbations propagate upward along the nearly vertical field lines of photospheric magnetic field concentrations with time-dependent local Alfvén speed, and thus can be identified as torsional Alfvén waves. This result also explains quasiperiodic oscillations and the short lifetimes of photospheric magnetic vortices, as noted by Moll et al. (2011) and Kitiashvili et al. (2013).

This Letter is structured as follows. In Section 2 we describe the simulation setup and the data we use for our analysis of photospheric vortices. The time–distance analysis of plasma motions in the upper-photospheric magnetic field concentrations is described in Section 3. Section 4 concludes our findings.

2. SIMULATION SETUP

The MURaM radiative MHD code (Vögler et al. 2005) has been used to carry out simulations of the magnetized solar photosphere. The code is well-tested, has demonstrated similar performance to other radiative MHD codes available in the community (Beeck et al. 2012), and has been widely used to provide an insight into the physical processes behind various solar observational phenomena, such as, for example, sunspots (Rempel et al. 2009), magnetic flux emergence (Cheung et al. 2008), and photospheric bright points (Schüssler et al. 2003; Shelyag et al. 2004). The code reproduces thermal and radiative properties of the solar photosphere well, as demonstrated by comparison of simulated photospheric spectral lines with observations (Shelyag et al. 2007).

For the analysis presented in this Letter we use the code setup described in detail by Shelyag et al. (2011b). The physical

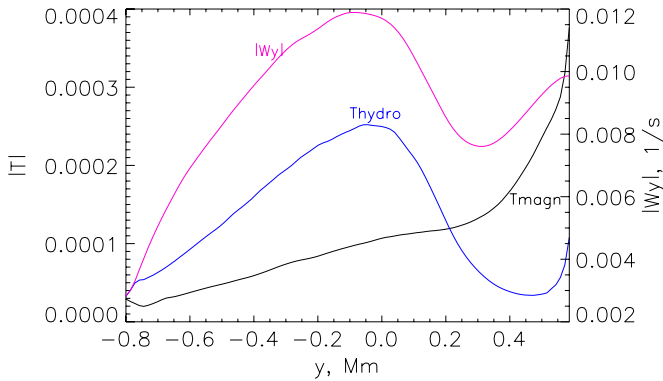


Figure 1. Dependences of the moduli of the vertical component of vorticity ($|W_y|$) and of magnetic (T_{magn}) and hydrodynamic (T_{hydro}) vorticity sources on height in Mm in the simulated solar photosphere. Here, negative values of y correspond to the convection zone, while positive values refer to the photosphere. (A color version of this figure is available in the online journal.)

domain size is $12 \times 12 \text{ Mm}^2$ in the horizontal directions and 1.4 Mm in the vertical direction, and the resolution is $25 \times 25 \text{ km}^2$ and 14 km , respectively. To generate the photospheric data, we introduce a uniform 200 G vertical magnetic field into a well-developed non-magnetic photospheric convection model, and, after the initial transient phase (about 40 minutes of physical time), we record 240 snapshots of photospheric model data with a mean cadence of 2.41 s . This short time step is required to capture processes at Alfvénic time scales in strongly magnetized regions of the solar photosphere where the characteristic speed can reach $50\text{--}100 \text{ km s}^{-1}$.

During the initial simulation phase, the magnetic field is advected into the intergranular lanes by convective motions, and photospheric magnetic flux concentrations with the strength of about 1.7 kG at the continuum formation height and of about 800 G in the upper photosphere are formed. Simultaneously, magnetic vortex structures appear in the low plasma β regions of the simulated solar atmosphere.

Figure 1 displays the dependences of absolute values of magnetic (black curve) and hydrodynamic (blue curve) sources in the vertical component of vorticity according to Equation (4) of Shelyag et al. (2011b), as well as the modulus of the vertical component of vorticity itself (pink curve), all averaged horizontally over the numerical domain. The figure shows that in the lower photosphere (below 0.2 Mm) the main source of vorticity is compressible fluid motion. Conversely, in the strongly magnetized upper photosphere (above 0.2 Mm), magnetic sources dominate over purely hydrodynamic vorticity sources. This clearly indicates that magnetic field effects are responsible for a strong increase in vertical vorticity above 0.3 Mm in the photosphere. Shelyag et al. (2011b) demonstrated that the vorticity source term, which contains magnetic tension, is responsible for this effect.

To visualize the three-dimensional velocity field in as simple and clear a manner as possible, we use a small number of seed particles that are randomly magnetic field-weight distributed around a magnetic field concentration over a horizontal plane close to the top boundary of the domain. This biases them toward the strong-field regions near the tube axis.

We first plot probe particle tracks under the action of the velocity field obtained from the first snapshot of the data series. An example of probe particle tracks under the action of this velocity field is shown in Figure 2. These are streamlines. As is evident from the figure, a vortex-like structure is present

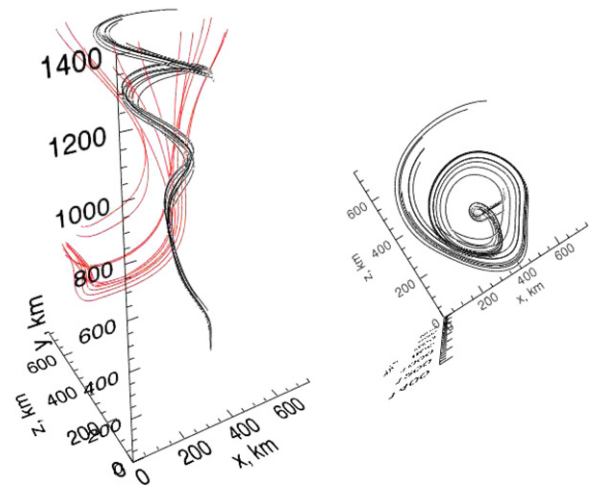


Figure 2. Probe particle tracks in the simulated photospheric magnetic field concentration under the action of the velocity field obtained from the first snapshot of the data series. Views from the side and from the top of the vortex structure are shown in left and right sides of the figure, respectively. Also, the magnetic field lines are plotted in gray (online version—red) in the left side of the figure. A fly-around animation of the left part of the figure is included in online material.

(An animation and a color version of this figure are available in the online journal.)

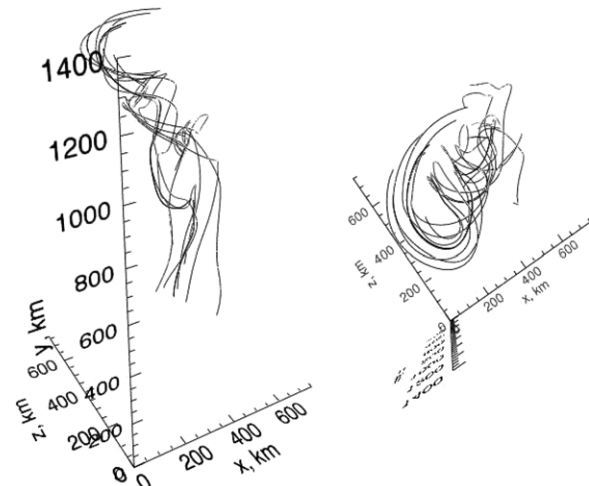


Figure 3. Probe particle tracks in the simulated photospheric magnetic field concentration under the action of the time-dependent velocity field over the simulation time series (about 500 s). A fly-around animation of the left part of the figure is included in online material.

(An animation of this figure is available in the online journal.)

in the upper part of the simulated photosphere. However, if the probe particles with the same initial coordinates are let to evolve in the time-dependent velocity field from the whole time series of the simulation, the upper-photospheric vortex completely disappears and is replaced by nearly random, quasi-oscillatory particle tracks (see Figure 3). These are pathlines. Streamlines and pathlines coincide only in steady flows. Their disparity clearly demonstrates that three-dimensional flow in upper-photospheric vortices in regions of strong magnetic field is far from steady. Moll et al. (2012) recently pointed out that the low twist of the magnetic field lines in their modeling indicates a non-stationary character of the flow. Indeed, the time scale for flow change is similar to the flow time scale itself. Thus, processes in the upper-photospheric magnetic vortices cannot

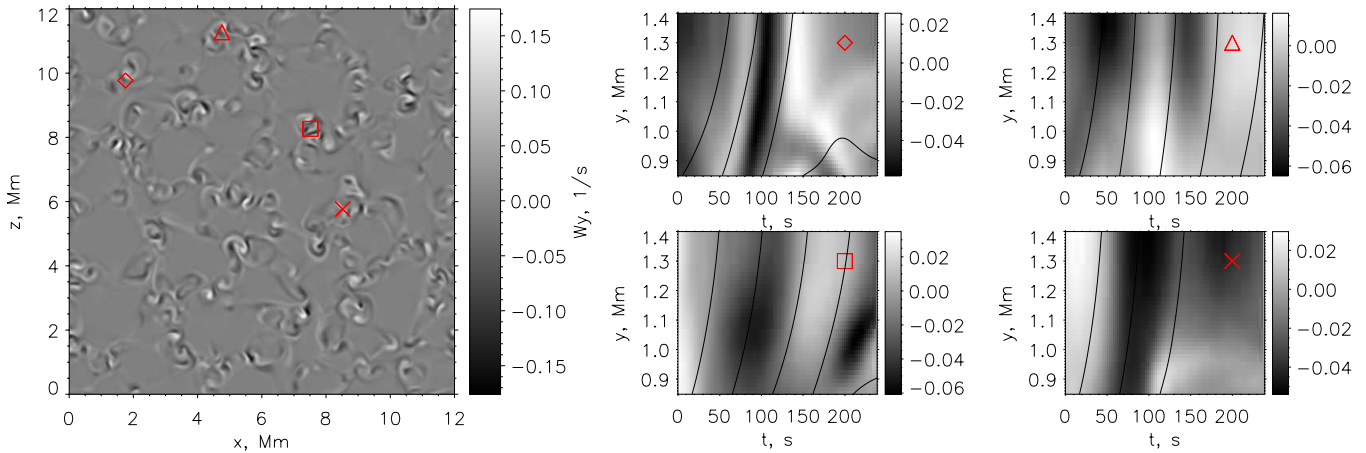


Figure 4. Upper photospheric vertical vorticity over a horizontal (x - z) plane at height about $y = 500$ km (left panel) and examples of time–distance diagrams of Alfvén wave propagation in the upper solar photosphere (right panels). The time–distance diagrams are measured along the vertical direction in the simulated solar photosphere at the positions marked by the symbols in the left panel. The curves plotted over the time–distance diagrams represent tracks for test particles under the action of local time-dependent Alfvén velocity. They are also corrected to account for the local time-dependent flow field.

(A color version of this figure is available in the online journal.)

be physically related to those in sinks or tornadoes in Earth’s atmosphere, where steady velocity fields are present. Vortical flow in a low-beta atmosphere cannot be sustained over many Alfvén crossing times unless it is an essentially solid-body rotation induced by rotational flows or flux tube unwindings in the high-beta layers below, since dominant magnetic tension will resist it.

In the following section, we confirm this finding with more detailed analysis of propagation of the vorticity perturbation through the solar atmosphere.

3. TIME–DISTANCE ANALYSIS OF VORTICITY IN PHOTOSPHERIC MAGNETIC FIELD CONCENTRATIONS

Basic analysis of the probe particle motions given in the previous section shows an absence of steady vortex flows in photospheric magnetic field concentrations. The presence of both vorticity signs, earlier reported by Shelyag et al. (2011a) and Steiner & Rezaei (2012), manifests both clockwise and anti-clockwise torsional motions within the same magnetic structure. This fact suggests wave-like motions of the plasma in photospheric magnetic field concentrations. To study these waves and to identify their types we perform time–distance analysis of the vorticity perturbation along the magnetic field lines in the simulated domain. Construction of time-dependent three-dimensional magnetic surfaces is a computationally difficult task, so we choose points where the magnetic field is nearly vertical in the neighborhood of the upper boundary of the domain.

Figure 4 shows a map of the vertical (y -)component of vorticity measured at about 500 km above the average continuum formation level (left panel), and four examples of time–distance diagrams of vertical propagation of the vertical component of vorticity. In choosing the examples, we restricted the selection to waves that propagate upwards only, though both upward and downward directions of wave propagation are observed. As is evident from the plots, all examples show oscillatory patterns of fast-propagating perturbations along the vertical direction. We were able to identify the wave type by overplotting the path for a test particle, which moves with the local, time-dependent Alfvén speed, according to the equation $\Delta y = \Delta t(\sqrt{B^2/4\pi\rho} + v_y)$ in cgs units, where v_y is local time-dependent vertical flow speed. The test particle tracks are plotted over the time–distance

diagrams and clearly coincide with the oscillatory pattern of the vertical component of the vorticity. Notably, the mean vertical flow speed averaged over the time series never exceeds 3 km s^{-1} , and the maximum vertical flow speed is about 6 km s^{-1} . Therefore, motions of the test particles with speed about 20 km s^{-1} cannot be explained by vertical plasma flows, as is evident from Figure 4. This finding demonstrates that the propagation speed for the vorticity perturbation is equal to the Alfvén speed. In the plots shown in the right part of Figure 4, the maximum magnetic field inclination angle in the time–distance region where a clear wave propagation pattern is observed is less than 10° . Therefore, the assumption about equivalence of propagation along the magnetic field line and along the vertical direction is well-justified. Summarizing the findings, the perturbation in the vertical component of the vorticity, that propagates vertically along magnetic field lines, is a horizontal torsional velocity perturbation, and thus it can be identified as a torsional Alfvén wave.

In fact, nearly all vertical columns in the regions of strong magnetic field in the simulation domain show propagation of a perturbation with speed close to the Alfvén speed. The abundance of these patterns in the computational domain and the nearly perfect agreement between the perturbation phase speed and the Alfvén speed also argue against advection of pre-existing vorticity patterns by horizontal bulk flows being the cause of the observed time–distance patterns. We conclude that torsional Alfvén waves originating in the higher photosphere are ubiquitous in plage regions of the solar photosphere.

4. CONCLUSIONS

In this Letter, we analyzed apparent photospheric magnetic vortex structures in a dynamic realistic simulation of solar photospheric magnetoconvection. We identified that no long-lived vortex structures in photospheric magnetic field concentrations exist. Instead, the time-dependent velocity field obtained from the simulations shows oscillatory behavior in the strong intergranular magnetic field regions. Using time–distance analysis of the vertical component of vorticity we found that the perturbations propagate vertically along the magnetic field lines with speeds equal to the local Alfvén speed. Thus we identified the perturbations as torsional Alfvén waves in intergranular

magnetic flux concentrations. In the structures shown in our simulations the velocity pattern changes within approximately 50 s to the opposite direction. This timescale is considerably shorter than the lifetime of the inter granular magnetic field concentrations which continue to exist throughout this process.

As our study shows, we must exercise caution when visualizing three-dimensional motions in the turbulent and magnetized solar atmosphere. Steady velocity fields cannot be used for analysis, since the speed with which the velocity pattern changes is of the same order as the actual velocity, while studies of time-dependent velocity fields impose additional requirements on the simulated data series, such as spatial resolution and cadence, as well as on the computational resources needed to perform the computations.

The vorticity perturbations we observe in the simulations, unlike pure Alfvén waves, cause perturbations in thermodynamic parameters of the solar plasma. These perturbations are possibly caused by some unavoidable amount of artificial diffusivity and resistivity included in the code for numerical stability. Another reason for these perturbations may be that other, magneto-acoustic oscillatory modes are present in the simulated magnetic field concentrations.

It also should be mentioned that, apparently, photospheric magnetic bright point motions, which originate at the base of the photosphere, do not represent good candidates for this type of wave observation, since they are formed deeper in photospheric layers (Shelyag et al. 2004; Carlsson et al. 2004). Their measured paths (Bonet et al. 2008) suggest a hydrodynamic, non-oscillatory type of photospheric horizontal motion.

Previous observational and theoretical reports on Alfvén waves in the solar chromosphere (e.g., Jess et al. 2009) and in sunspots (Brown et al. 2003; Khomenko & Cally 2012) clearly suggest that Alfvén waves are a common phenomenon in strong solar magnetic fields. Interestingly, recent high-cadence observations of prominences show that their tornado-like appearance is “an illusion due to projection effects” (Panasenco et al. 2013), suggesting a general presence of Alfvén-type motions in the solar atmosphere and corona.

Observational confirmation of the result given in this Letter is currently rather difficult since it requires spectroscopic and spectropolarimetric observations with both very high resolution of the order of 20–50 km and extremely high cadence of about 2 s. These may become possible with upcoming high-aperture instruments, such as ATST. Further investigation of the reaction of spectral line profiles to photospheric Alfvén waves will be needed before such an observational attempt.

Another interesting problem is detailed identification of the lower-photospheric sources of upper-photospheric torsional waves. Among the possibilities are hydrodynamic vortices in the deep photosphere, small-scale granular motions and short-lived

turbulent eddies. Further theoretical and computational work is needed to fully determine the sources of Alfvén waves observed in the upper photosphere.

This research was undertaken with the assistance of resources provided at the NCI National Facility systems at the Australian National University through the National Computational Merit Allocation Scheme supported by the Australian Government, and at the Multi-modal Australian ScienceS Imaging and Visualisation Environment (MASSIVE) (www.massive.org.au). The authors also thank Centre for Astrophysics & Supercomputing of Swinburne University of Technology (Australia) for the computational resources provided. Dr. Shelyag is the recipient of an Australian Research Council’s Future Fellowship (project number FT120100057).

REFERENCES

- Beeck, B., Collet, R., Steffen, M., et al. 2012, *A&A*, **539**, A121
- Bonet, J. A., Márquez, I., Sánchez Almeida, J., Cabello, I., & Domingo, V. 2008, *ApJL*, **687**, L131
- Brown, D. S., Nightingale, R. W., Alexander, D., et al. 2003, *SoPh*, **216**, 79
- Carlsson, M., Stein, R. F., Nordlund, Å., & Scharmer, G. B. 2004, *ApJL*, **610**, L137
- Cheung, M. C. M., Schüssler, M., Tarbell, T. D., & Title, A. M. 2008, *ApJ*, **687**, 1373
- Fedun, V., Shelyag, S., Verth, G., Mathioudakis, M., & Erdélyi, R. 2011, *AnGeo*, **29**, 1029
- Freytag, B., Steffen, M., Ludwig, H.-G., et al. 2012, *JCoPh*, **231**, 919
- Jess, D. B., Mathioudakis, M., Erdélyi, R., et al. 2009, *Sci*, **323**, 1582
- Khomenko, E., & Cally, P. S. 2012, *ApJ*, **746**, 68
- Kitiashvili, I. N., Kosovichev, A. G., Lele, S. K., Mansour, N. N., & Wray, A. A. 2013, *ApJ*, **770**, 37
- Moll, R., Cameron, R. H., & Schüssler, M. 2011, *A&A*, **533**, A126
- Moll, R., Cameron, R. H., & Schüssler, M. 2012, *A&A*, **541**, A68
- Morton, R. J., Verth, G., Fedun, V., Shelyag, S., & Erdélyi, R. 2013, *ApJ*, **768**, 17
- Panasenco, O., Martin, S. F., & Velli, M. 2013, *SoPh*, in press
- Rempel, M., Schüssler, M., Cameron, R. H., & Knölker, M. 2009, *Sci*, **325**, 171
- Schüssler, M., Shelyag, S., Berdyugina, S., Vögler, A., & Solanki, S. K. 2003, *ApJL*, **597**, L173
- Shelyag, S., Fedun, V., Keenan, F. P., Erdélyi, R., & Mathioudakis, M. 2011a, *AnGeo*, **29**, 883
- Shelyag, S., Keys, P., Mathioudakis, M., & Keenan, F. P. 2011b, *A&A*, **526**, A5
- Shelyag, S., Mathioudakis, M., & Keenan, F. P. 2012, *ApJL*, **753**, L22
- Shelyag, S., Schüssler, M., Solanki, S. K., Berdyugina, S. V., & Vögler, A. 2004, *A&A*, **427**, 335
- Shelyag, S., Schüssler, M., Solanki, S. K., & Vögler, A. 2007, *A&A*, **469**, 731
- Steiner, O., & Rezaei, R. 2012, in ASP Conf. Ser. 456, The Fifth Hinode Science Meeting, ed. L. Golub, I. De Moortel, & T. Shimizu (San Francisco, CA: ASP), 3
- Vögler, A. 2004, in The Sun and Planetary Systems—Paradigms for the Universe, ed. E. Schielicke (Reviews in Modern Astronomy, Vol. 17; Weinheim: Wiley), 69
- Vögler, A., Shelyag, S., Schüssler, M., et al. 2005, *A&A*, **429**, 335
- Wedemeyer-Böhm, S., & Rouppe van der Voort, L. 2009, *A&A*, **507**, L9
- Wedemeyer-Böhm, S., Scullion, E., Steiner, O., et al. 2012, *Natur*, **486**, 505